C_2-Symmetric *Ansa*-Lanthanidocene Complexes. Theoretical Evidence for a Symmetric Ln···(Si−H) β-Diagostic Interaction

Wolfgang Hieringer, Jörg Eppinger, Reiner Anwander, and Wolfgang A. Herrmann*

Contribution from the Anorganisch-chemisches Institut, Technische Universität München, Lichtenbergstrasse 4, D-85747 Garching, Germany

Received September 20, 1999. Revised Manuscript Received June 15, 2000

Abstract: Density functional calculations on *ansa*-bridged rare earth disilylamide complexes confirm the presence of a new type of symmetric Ln···(Si−H) β-diagostic interaction, the origin and electronic structure of which are delineated in terms of structural criteria, vibrational spectra, natural population analyses, natural bond orbitals, and canonical molecular orbitals. The interaction turns out to be dominated by electrostatic effects, and the presence of vacant f orbitals appears to be of minor importance for the bonding in this case. It is shown that only central metals of sufficient size allow for a diagostic coordination mode due to steric hindrance.

1. Introduction

In a number of transition metal complexes, C−H bonds of alkyl or alkenyl ligands can bind to the metal center, acting formally as a two-electron donor. Brookhart and Green coined the term "agostic" for this type of interaction.[1] Since then, the meaning of the word "agostic" has been used not only for C−H groups, but also for a variety of unusual (Si−H)···TM (TM = transition metal) interactions.[2,3] Agostic bonding has been found to play a major role in the ligand reactivity of transition metal complexes, particularly in α-olefin polymerization.[4,5]

The nature of the interaction was interpreted by Brookhart and Green in terms of a three-center, two-electron bond between the C−H bond and a vacant d orbital of the transition metal, leading to a charge transfer from the C−H σ bond to the metal.[1] When performing a formal electron count, one can regard the agostic ligand as a whole as a four-electron ligand, with two electrons being donated by the carbon atom of the M−C bond and another two electrons by the C−H group. However, recent theoretical studies on ethyltitanium trichloride suggest that only one doubly occupied molecular orbital is responsible for the overall bonding of the ligand to the metal, the ligand thus formally acting as a two-electron ligand.[6]

The presence of an agostic interaction is commonly proved by the resulting geometrical deformations of the agostic ligand, which are mainly an elongation of the E−H bond (E = C, Si), rather short M···H contacts, and a distortion of the ligand geometry toward the metal center.[1,7] In a variety of X-ray crystal structure analyses, hydrogen atoms were located and refined to provide an estimation of their positions.[2,3] More precise data were collected using neutron and electron diffraction techniques.[8,9] IR spectroscopy was applied to document the weakening of the agostic C−H bond by a low-frequency shift of the corresponding band.[10] The proximity of the metal center was also shown by characteristic NMR chemical shifts of agostic protons and concomitant reduction of the J_{CH} coupling constant.[2b]

(1) (a) Brookhart, M.; Green, M. L. H. *J. Organomet. Chem.* **1983**, *250*, 395−408. (b) Brookhart, M.; Green, M. L. H.; Wong, L.-L. *Prog. Inorg. Chem.* **1988**, *36*, 1−124.

(2) (a) Hoyano, J. K.; Elder, M.; Graham, W. A. G. *J. Am. Chem. Soc.* **1969**, *91*, 4568−4569. (b) Carré, F.; Colomer, E.; Corriu, R. J. P.; Vioux, A. *Organometallics* **1984**, *3*, 1272−1278. (c) Spaltenstein, E.; Palma, P.; Kreutzer, K. A.; Willoughby, C. A.; Davis, W. M.; Buchwald, S. L. *J. Am. Chem. Soc.* **1994**, *116*, 10308−10309. (d) Procopio, L. J.; Carroll, P. J.; Berry, D. H. *J. Am. Chem. Soc.* **1994**, *116*, 177−185. (e) Luo, X.-L.; Kubas, G. J.; Bryan, J. C.; Burns, C. J.; Unkefer, C. J. *J. Am. Chem. Soc.* **1994**, *116*, 10312−10313. (f) Ohff, A.; Kosse, P.; Baumann, W.; Tillack, A.; Kempe, R.; Görls, H.; Burlakov, V. V.; Rosenthal, U. *J. Am. Chem. Soc.* **1995**, *117*, 10399−10400. (g) Fan, M.-F.; Jia, G.; Lin, Z. *J. Am. Chem. Soc.* **1996**, *118*, 9915−9921. (h) Delpech, F.; Sabo-Etienne, S.; Chaudret, B.; Daran, J.-C. *J. Am. Chem. Soc.* **1997**, *119*, 3167−3168. (i) Peulecke, N.; Ohff, A.; Kosse, P.; Tillack, P.; Spannenburg, A.; Kempe, R.; Baumann, W.; Burlakov, V. V.; Rosenthal, U. *Chem. Eur. J.* **1998**, *4*, 1852−1861. (j) Delpech, F.; Sabo-Etienne, S.; Daran, J.-C.; Chaudret, B.; Hussein, K.; Marsden, C. J.; Barthelat, J.-C. *J. Am. Chem. Soc.* **1999**, *121*, 6668−6682. (k) For a review, see: Schubert, U. *Adv. Organomet. Chem.* **1990**, *30*, 151−187.

(3) (a) Rees, W. S., Jr.; Just, O.; Schumann, H.; Weinmann, R. *Angew. Chem., Int. Ed. Engl.* **1996**, *35*, 419−422. (b) Herrmann, W. A.; Eppinger, J.; Spiegler, M.; Runte, O.; Anwander, R. *Organometallics* **1997**, *16*, 1813−1815. (c) Nagl, I.; Scherer, W.; Tafipolsky, M.; Anwander, R. *Eur. J. Inorg. Chem.* **1999**, 1405−1407.

(4) (a) Grubbs, R. H.; Coates, G. W. *Acc. Chem. Res.* **1996**, *29*, 85−93. (b) Piers, W. J.; Bercaw, J. E. *J. Am. Chem. Soc.* **1990**, *112*, 9406−9407. (c) Burger, B. J.; Thompson, M. E.; Cotter, W. D.; Bercaw, J. E. *J. Am. Chem. Soc.* **1990**, *112*, 1566−1577.

(5) (a) Margl, P.; Lohrenz, J. C. W.; Ziegler, T.; Blöchl, P. E. *J. Am. Chem. Soc.* **1996**, *118*, 4434−4441. (b) Cooper, A. C.; Huffman, J. C.; Folting, K.; Caulton, K. G. *Organometallics* **1996**, *15*, 3990−3997.

(6) Haaland, A.; Scherer, W.; Ruud, K.; McGrady, G. S.; Downs, A. J.; Swang, O. *J. Am. Chem. Soc.* **1998**, *120*, 3762−3772.

(7) Dawoodi, Z.; Green, M. L. H.; Mtetwa, V. S. B.; Prout, K. *J. Chem. Soc., Chem. Commun.* **1982**, 802−803.

(8) For neutron diffraction studies, see: (a) Klooster, W. T.; Lu, R. S.; Anwander, R.; Evans, W. J.; Koetzle, T. F.; Bau, R. *Angew. Chem., Int. Ed.* **1998**, *37*, 1268−1270. (b) Klooster, W. T.; Brammer, L.; Schaverien, C. J.; Budzelaar, P. H. M. *J. Am. Chem. Soc.* **1999**, *121*, 1381−1382. (c) Hitchcock, P. B.; Howard, J. A. K.; Lappert, M. F.; Leung, W.-P.; Mason, S. A. *J. Chem. Soc., Chem. Commun.* **1990**, 847−849. (d) Rhine, W. E.; Stucky, G.; Peterson, S. W. *J. Am. Chem. Soc.* **1975**, *97*, 6401−6406. (e) Dawoodi, Z.; Green, M. L. H.; Mtetwa, V. S. B.; Prout, K.; Schultz, A. J.; Williams, J. M.; Koetzle, T. F. *J. Chem. Soc., Dalton Trans.* **1986**, 1629−1637.

(9) For an electron diffraction study, see: Berry, A.; Dawoodi, Z.; Derome, A. E.; Dickinson, J. E.; Dowens, A. J.; Green, J. C.; Green, M. L. H.; Hare, P. M.; Payne, P. M.; Rankin, D. W. H.; Robertson, H. E. *J. Chem. Soc., Chem. Commun.* **1986**, 520−522.

(10) (a) McGrady, G. S.; Downs, A. J.; Haaland, A.; Scherer, W.; McKean, D. C. *J. Chem. Soc., Chem. Commun.* **1997**, 1547−1548. (b) Barnhart, D. M.; Clark, D. L.; Gordon, J. C.; Huffman, J. C.; Watkin, J. G.; Zwick, B. D. *J. Am. Chem. Soc.* **1993**, *115*, 8461−8462. (c) See also: McKean, D. C.; McQuillan, G. P.; Torto, I.; Morrison, A. R. *J. Mol. Struct.* **1986**, *141*, 457−464.

10.1021/ja993421t CCC: $19.00
Published on Web 11/11/2000

In some cases, proton−metal spin−spin coupling was observed.[3b] Paralleling experimental studies, efforts were made to understand agostic bonds by theoretical methods. Extended Hückel molecular orbital calculations by Hoffmann[11] and Eisenstein[12] provided insight into the bonding mechanisms of this type of interaction. Later, structural, spectroscopic, and bonding features were confirmed and refined by high-level ab initio and density functional calculations.[6,13] In principle, such calculations have an advantage over X-ray crystallography in that hydrogen positions are known exactly within the accuracy of the model chemistry used.

In recent years, several complexes with agostic Si−H···TM interactions have appeared in the literature.[2,3] The very few known examples of rare earth metals invariably comprise silylamide ligands, all of them showing unusual multiple agostic coordination modes.[3] In an earlier paper, a new type of symmetric Ln···(Si−H) β-diagostic interaction observed in a number of rare earth metal complexes **A** was reported and characterized by X-ray crystallography and spectroscopic methods.[14] The peculiar coordination modes in combination with

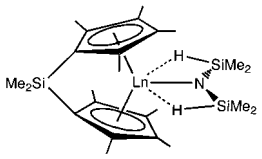

A

the common notion that rare earth metals tend to favor purely ionic interactions[15] makes this class of complexes particularly interesting for theoretical investigations.

The purpose of this paper is to provide insight into the electronic structure and the unprecedented agostic bonding mode in **A**, modeled as *ansa*-bridged rare earth disilylamide complexes **1**−**3** (Scheme 1) using current density functional methods.[16] Structural and spectroscopic features are used to delineate the characteristics of this interaction. We wish to clarify whether low-lying f orbitals can participate in the bonding mechanism and investigate the degree of covalent and electrostatic contributions to the bonding. We are furthermore interested in the energy that is associated with the agostic interaction, which might act chemically as a ligand, screening the metal center from solvent coordination, bearing important synthetic consequences. Finally,

Scheme 1. Structural Models of Agostic Bonding in **1**−**7**

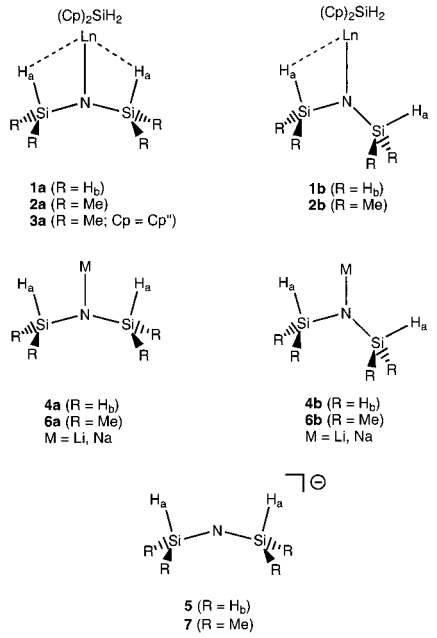

we look for criteria, such as rare earth metal ionic radius, allowing for the formation of a symmetric diagostic rather than a monoagostic bond.

2. Computational Details

Density functional theory with gradient-corrected exchange correlation functionals has proved to be a reliable tool for performing electronic structure calculations on transition metal complexes at a moderate cost.[16] The calculations presented in this study have been carried out using the 1988 gradient-corrected exchange in combination with the 1986 correlation functional introduced by Becke[17a] and Perdew[17b] (BP86). This functional combination has yielded the best agreement with experimental data in our case. More details on the performance of other levels of theory can be found in the Supporting Information.

Despite the efficiency of Kohn−Sham density functional theory as compared to post-Hartree−Fock methods, the size of the complexes tackled here led us to seek the most economic way to treat the problem accurately. The most proven method for large transition metal complexes is the use of pseudorelativistic effective core potentials,[18,19] which allows us to deal with the valence electrons exclusively. All model complexes were treated using effective small-core potentials on the rare earth and silicon atoms together with a Gaussian valence basis set of double-ζ (triple-ζ for Lu) quality.[20] Los Alamos ECPs[18] (LanL2DZ) were used for Sc, Y, La and Si, while an ECP optimized by the Stuttgart[19] group was used for Lu. The orbital basis sets on the disilylamide fragment were augmented by a single set of polarization functions according to Huzinaga,[21] i.e., one set of p functions on each of the six (two in case of $N(SiHMe_2)_2$) hydrogen atoms of the SiH_3 groups, one set of d functions on nitrogen, and one set of appropriate d-type Gaussians on each of the silicon atoms, yielding a basis set labeled DZP in this paper. An additional set of f-type polarization functions according to Frenking[22] was furthermore added on the Sc, Y, and La centers (basis set label DZP+f). For Lu, an f function exponent of 0.772 was used within DZP+f.

(11) (a) Goddard, R. J.; Hoffmann, R.; Jemmis, E. D. *J. Am. Chem. Soc.* **1980**, *102*, 7667−7676. (b) Saillard, J.-Y.; Hoffmann, R. *J. Am. Chem. Soc.* **1984**, *106*, 2006−2026.

(12) (a) Eisenstein, O.; Jean Y. *J. Am. Chem. Soc.* **1985**, *107*, 1177−1186. (b) Cauchy, D.; Eisenstein, O.; Jean, Y.; Volatron, F. *New J. Chem.* **1994**, *18*, 687−691.

(13) (a) Francl, M. M.; Pietro, W. J.; Hout, R. F.; Hehre, W. J. *Organometallics* **1983**, *2*, 281−286. (b) Obara, S.; Koga, N.; Morokuma, K. *J. Organomet. Chem.* **1984**, *270*, C33−C36. (c) Koga, N.; Obara, S.; Morokuma, K. *J. Am. Chem. Soc.* **1984**, *106*, 4625−4626. (d) Koga, N.; Morokuma, K. *J. Am. Chem. Soc.* **1988**, *110*, 108−112. (e) Fan, M.-F.; Jia, G.; Lin, Z. *J. Am. Chem. Soc.* **1996**, *118*, 9915−9921. (f) Maseras, F.; Lledós, A. *Organometallics* **1996**, *15*, 1218−1222. (g) Fan, M.-F.; Lin, Z. *Organometallics* **1997**, *16*, 494−496. (h) For comparison, see: Williams, R. L.; Hall, M. B. *J. Am. Chem. Soc.* **1988**, *110*, 4428−4429.

(14) Eppinger, J.; Spiegler, M.; Hieringer, W.; Herrmann, W. A.; Anwander, R. *J. Am. Chem. Soc.* **2000**, *122*, 3080−3096.

(15) (a) Strittmatter, R. J.; Bursten, B. E. *J. Am. Chem. Soc.* **1991**, *113*, 552−559. (b) Burns, C. J.; Bursten, B. E. *Comments Inorg. Chem.* **1989**, *9*, 61−93.

(16) (a) Ziegler, T. *Chem. Rev.* **1991**, *91*, 651−667. (b) Fan, L.; Ziegler, T. *J. Chem. Phys.* **1991**, *95*, 7401−7408. (c) Kohn, W.; Becke, A. D.; Parr, R. G. *J. Phys. Chem.* **1996**, *100*, 12974−12980. (d) Andzelm, J.; Labanowski, J. *Density Functional Methods in Chemistry*; Springer-Verlag: Heidelberg, 1991. (e) Parr, R. G.; Yang, W. *Density Functional Theory of Atoms and Molecules*; Oxford University Press: Oxford, UK, 1991.

(17) (a) Becke, A. D. *Phys. Rev. A* **1988**, *38*, 3098−3100. (b) Perdew, J. P. *Phys. Rev. B* **1986**, *33*, 8822−8824; **1986**, *34*, 7406 (Erratum).

(18) (a) Hay, P. J.; Wadt, W. R. *J. Chem. Phys.* **1985**, *82*, 270−283. (b) Wadt, W. R.; Hay, P. J. *J. Chem. Phys.* **1985**, *82*, 284−298. (c) Hay, P. J.; Wadt, W. R. *J. Chem. Phys.* **1985**, *82*, 299−310.

(19) (a) Dolg, M.; Stoll, H.; Savin, A.; Preuss, H. *Theor. Chim. Acta* **1989**, *75*, 173−194. (b) Dolg, M.; Stoll, H.; Preuss, H. *J. Chem. Phys.* **1989**, *90*, 1720−1734.

(20) Dunning, T. H.; Hay, P. J. In *Modern Theoretical Chemistry*; Schaefer, H. F., III, Ed.; Plenum: New York, 1976; pp 1−28.

(21) Huzinaga, S. *Gaussian Basis Sets for Molecular Calculations*; Elsevier: Amsterdam, 1984.

Table 1. Selected Structural Parameters for Optimized Structures in Angstroms and Degrees (BP86)

compound/method	∠Si−N−Si	Si−H_a	Si−H_b	∠H_a−Si−N	∠H_b−Si−N	M···H_a
experimental[a]	154.88(18)	1.39(3)[b]		102.4(13)		2.70(3)[b]
		1.38(4)[b]		100.7(16)		2.66(4)[b]
1a (La) DZP	155.8	1.538	1.489	102.1	117.4	2.68
1a (La) DZP+f	154.5	1.536	1.488	101.8	117.3	2.68
2a (La) DZP	159.6	1.556		100.3		2.58
2a (La) DZP+f	158.2	1.552		100.0		2.58
3a (La) DZP	156.5	1.552		101.0		2.67
3a (La)DZP+f	155.5	1.548		100.7		2.66
4a (Li) DZP	132.1	1.508	1.497	107.4	115.9	2.89
4b (Li) DZP	132.8	1.538/1.496[c]	1.495/1.497[c]	102.4/109.7[c]	118.8/114.5[c]	2.14/3.48[c]
4a (Na) DZP	134.7	1.514	1.501	108.0	134.7	3.05
4b (Na) DZP	132.1	1.531/1.503[c]	1.500/1.501[c]	105.9/109.8[c]	118.4/115.7[c]	2.52/3.62[c]
5 DZP	148.6	1.515	1.523	113.8	118.2	
6a (Li) DZP	175.9	1.561		102.5		2.10
6a (Na) DZP	165.1	1.551		105.5		2.48
6b (Li) DZP	141.0	1.560/1.507[c]		100.4/107.4[c]		2.02/3.28[c]
7 DZP	177.1	1.521		115.2		

[a] Reference 14, compound **11c** (Ln = La). [b] La···H and Si−H distances have to be discussed carefully due to the uncertainty of location of the hydrogen atoms close to two heavy atoms. [c] Left/right value: silyl group close to/far from the metal center.

Full geometry optimizations were carried out in C_1 symmetry using analytical gradient techniques, and the resulting structures were confirmed to be true minima by diagonalization of the analytical nuclear Hessian matrix.[23] All molecular orbital (MO), natural bond orbital (NBO), and natural population (NPA) analyses[24] were performed within the BP86/DZP+f level. For the model compounds M[N($SiHR_2$)$_2$] **4a/b** (R = H, M = Li, Na)), **6a/b** (R = Me, M = Li, Na), and [N($SiHR_2$)$_2$]$^-$ **5/7** (R = H, Me), the DZP basis set was employed. Here, geometry optimizations were carried out in C_{2v} or C_s symmetry, unless stated otherwise. All calculations presented were performed using the Gaussian 98 program suite.[25] Molecular orbital plots were made with the Molden graphical interface.[26]

3. Results and Discussion

3.1. Geometry Optimization of Different Structural Models. *Ansa*-lanthanidocene bis(dimethylsilyl)amide complexes **A** have been studied in an earlier contribution[14] by X-ray crystallography and spectroscopic methods. Several structural peculiarities in these complexes point to the presence of a pronounced Si−H···Ln (Ln = La, Y, Lu, Sc) interaction, which will be examined by virtue of several model structures in this work. In the first part of the paper, we will deal exclusively with the lanthanum complexes, and we will extend our study to scandium, yttrium, and lutetium later.

To keep the computations feasible, we have simplified the experimental structures **A** to model structure [H_2Si(Cp)$_2$LnN(SiH_3)$_2$] **1** that is believed to represent a fair approximation of the electronic situation of the lanthanum center and the agostic Si−H groups. When comparing experimental structures with the calculated structures **1**, one has to keep in mind that steric effects are, of course, not modeled adequately with this procedure. To estimate the limitations of model compounds **1**, we performed additional calculations on complex **2** bearing the real N($SiHMe_2$)$_2$ (bdsa) ligand, as well as on [H_2Si(Cp'')$_2$LaN($SiHMe_2$)$_2$] **3** (Cp'' = C_5Me_4), which takes into account the substitution of the cyclopentadienyl rings. The main focus of this paper is on the electronic nature of the observed diagostic interaction, however.

Initial Geometries and Symmetry. There are basically three coordination modes of the disilylamide (dsa, bdsa) ligand to the metal center, featuring zero (nonagostic), one (monoagostic), or two close hydrogen lanthanum contacts (diagostic) (Scheme 1). The first and the last (structure type **1a/2a/3a**) formally show C_{2v} symmetry, while structures **1b/2b** display C_s symmetry. When investigating compounds of type **1a/2a/3a**, we adopted initial geometrical data from the X-ray structure of complex **A** (Ln = La).[14] The approximate C_{2v}-symmetric diagostic structure is the only coordination mode observed experimentally in compounds **A** for larger rare earth metals such as La and in the absence of steric constraints. Despite this fact, we also wanted to check about the possibility and properties of equilibrium structures such as **1b** or **2b**. To obtain a suitable starting structure, we "broke" one of the agostic bonds in **1a**/**2a** by asymmetrically contracting the Si−N−Si angle to 130°. The resulting starting structure was then also subjected to unconstrained geometry optimization, the results of which are presented in the following sections.

Comparison with Experimental Data. Critical parameters of the optimized structures describing the La···H distance, Si−N−Si and H−Si−N angles, as well as Si−H bond lengths, are compiled in Table 1.

The characteristic agostic distortions of the local $SiHR_2$ geometry, namely elongation of the agostic Si−H_a bonds and N−Si−H_a angle contraction, are common features of all structural models (Scheme 2). However, comparison of these results with the experimental data has to be done with care, since hydrogen positions are not known exactly from X-ray structure determination. Therefore, to benchmark the accuracy of theoretical predictions and the quality of the structural models, we regard the Si−N−Si angle as the single critical parameter to compare with experiment. The widening of the Si−N−Si

(22) Ehlers, A. W.; Böhme, M.; Dapprich, S.; Gobbi, A.; Höllwarth, A.; Jonas, V.; Köhler, K. F.; Stegmann, R.; Veldkamp, A.; Frenking, G. *Chem. Phys. Lett.* **1993**, *208*, 111−114.

(23) Komornicki, A.; Fitzgerald, G. *J. Chem. Phys.* **1993**, *98*, 1398−1421.

(24) (a) Reed, A. E.; Weinhold, F.; Weiss, R.; Macheleid, J. *J. Phys. Chem.* **1985**, *89*, 2688−2694. (b) Reed, A. E.; Curtiss, L. A.; Weinhold, F. *Chem. Rev.* **1988**, *88*, 899−926. (c) Foster, J. P.; Weinhold, F. *J. Am. Chem. Soc.* **1980**, *102*, 7211−7218. (d) Reed, A. E.; Weinhold, F. *J. Chem. Phys.* **1983**, *78*, 4066−4073. (e) Reed, A. E.; Weinstock, R. B.; Weinhold, F. *J. Chem. Phys.* **1985**, *83*, 735−746. (f) Reed, A. E.; Weinhold, F. *J. Chem. Phys.* **1985**, *83*, 1736−1740. (g) The NBO transformation of **1a** at BP86/DZP+f resulted in the following decomposition: total Lewis, 176.59 (97.0%); valence non-Lewis, 5.14 (2.83%); Rydberg non-Lewis, 0.28 (0.151%) of 182 electrons.

(25) Frisch, M. J.; Trucks, G. W.; Schlegel, H. B.; Gill, P. M. W.; Johnson, B. G.; Robb, M. A.; Cheeseman, J. R.; Keith, T. A.; Peterson, G. A.; Montgomery, J. A.; Raghavachari, K.; Al-Laham, M. A.; Zakrzewski, V. G.; Ortiz, J. V.; Foresman, J. B.; Cioslowski, J.; Stefanov, B. B.; Nanayakkara, A.; Challacombe, M.; Peng, C. Y.; Ayala, P. Y.; Chen, W.; Wong, M. W.; Andres, J. L.; Replogle, E. S.; Gomperts, R.; Martin, R. L.; Fox, D. J.; Binkley, J. S.; Defrees, D. J.; Baker, J.; Stewart, J. P.; Head-Gordon, M.; Gonzalez, C.; Pople, J. A. *Gaussian 98*, Revisions A.3 and A.7; Gaussian, Inc.: Pittsburgh, PA, 1998.

(26) Schaftenaar, G. CAOS/CAMM Center, University of Nijmegen, NL.

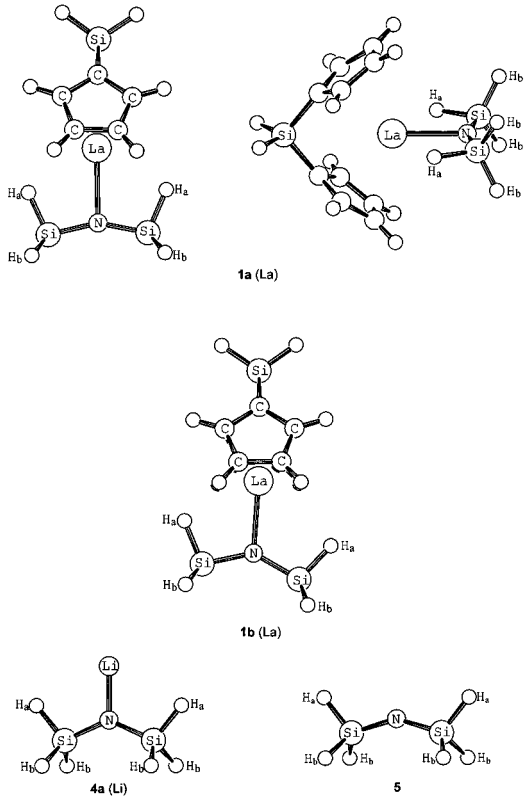

Figure 1. Optimized geometries of **1a**, **1b**, **4a**, and **5**.

Scheme 2. Agostic Distortions

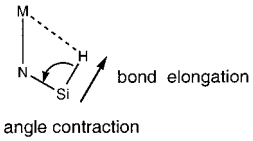

angle is the crucial structural evidence of a β-diagostic interaction which can be taken from the X-ray structure.

As can be seen from Table 1, this parameter is generally well reproduced by theory, with minor variations among the different models. From a theoretical point of view, it is interesting to see that inclusion of f basis functions into the basis set of the rare earth metal improves the agreement only slightly. This points to the fact that f orbitals probably do not play a central role in the formation of the double agostic bond, as will be underlined in subsequent sections.[27]

The good agreement with the experimental structure **A** is interesting in view of the structural simplifications made in model compound **1a** (Figure 1), i.e., omission of the four methyl groups of the real bdsa ligand. As can be seen from Table 1, the four methyl groups in **2** lead to a slightly more opened Si−N−Si angle of 158.2°. Together with other structural features (Table 1), this points to an enhanced agostic interaction in **2**. The closed-shell repulsion of the Me groups and different electronics within the bdsa moiety may also favor wider Si−N−Si angles, as can be seen from the geometries of the isolated dsa (**5**) and bdsa (**7**) ligands.

While the Si−N−Si angle in **2** compares slightly worse with the experimental reference, excellent agreement is restored when the methyl substituents on the cyclopentadienyl rings are taken into account as in **3**. This can be rationalized by steric repulsion of the Cp″ rings and the Me groups of the bdsa ligand. Alternatively, one could argue that the enhanced donating power of the methyl-substituted Cp″ compared to Cp reduces the electrophilicity of the central metal. In summary, however, we conclude that the geometrical perturbations due to methyl substitution are modest, and the simpler model **1** constitutes a sufficient starting point to study the origin and electronic properties of the double agostic interaction in compounds **A**. The excellent agreement of the Si−N−Si angle with the experimental data is, in part, the result of error cancellation, as indicated above. We like to point out here that the comparison with an experimental X-ray structure bears certain dangers, since crystal packing effects might influence the result.

An important question of our investigation was whether there also exists an asymmetric minimum structure in addition to the observed symmetric one. Hence, we were looking for a C_s-symmetric minimum structure of type **1b** with one long and one short La···H_a distance. Such a structure could not be located using the standard methods employed in this study (BP86/DZP, BP86/DZP+f). This also holds for the bdsa-containing structures **2**, where attempts to minimize initial geometries of type **2b** resulted in equilibrium structures **2a**. This is not surprising, given the enhanced strength of agostic bonding in **2**. A local minimum structure **1b**, however, was found at a lower level of theory (BP86/LanL2DZ), which serves as an approximation to a hypothetical structure **1b** in the following discussion. We cannot, however, rigorously rule out the existence of a minimum structure **1b** at higher levels, since we did not scan the potential hypersurface completely. The nonexistence of structure **1b** (La) (Figure 1) at high levels of theory parallels the experimental observations, where only a diagostic complex of lanthanum was detected so far.

In structure **1b** obtained as described, the silyl group next to the lanthanum center is strongly distorted, while the silyl group on the far side of the metal is nearly unperturbed. The Si−N−Si angle is markedly reduced (138.6°) as compared to that in the symmetric diagostic structures **1a**.

To obtain deeper insight into the bonding mechanism, we additionally optimized several model structures **4** and **6**, where the {H_2SiCp_2La} fragment was replaced simply by the alkali metals lithium or sodium (Scheme 1). Comparison of the properties of these compounds with those of the rare earth complexes allows us to estimate the role of electrostatic effects in the agostic bonding in later sections of this report. Relevant structural parameters have been included in Table 1. At this moment, we would like to note only that the C_{2v}-symmetric structures **4a**/**6a** (Li, Na) represent transition states with respect to a reduction of symmetry to yield minimum structures **4b**/**6b** of C_s symmetry. The only exception is the sodium-containing compound **6a** (Na), where no asymmetric structure **6b** could be located at the theoretical level used, paralleling the observations for the lanthanum complexes **1** and **2**.

Agostic Silyl Group Distortion. We now come back to the point of how the local geometry of the $SiHR_2$ (R = H, Me) groups changes upon formation of the agostic bonds by means of a more quantitative discussion. To compare the structures of the rare earth complexes **1**, **2**, and **3** with the geometry of nonagostic disilylamide fragments, we make use of our model compounds **4**−**7**. Compounds **4** and **6** are considered as the limiting case of a weak, predominantly ionic metal hydrogen interaction,[28] whereas in **5** and **7** no metal influence is present at all.

In the C_{2v}-symmetric structure **1a**, the agostic Si−H_a bonds are stretched by 0.05 Å with respect to their nonagostic counterparts Si−H_b. An analogous, but more subtle elongation

(27) A more elaborate study on the performance of different computational levels can be found in the Supporting Information.

Table 2. Si−H Stretching Vibrational Frequencies (cm^{-1}; Totally Symmetric Modes; BP86/DZP+f, Unscaled)

vibration	La	Y	Sc	Lu	Li	Na
dsa, Si−H_a	1948 (**1a**)	1939 (**1a**)		1921 (**1a**)[b]	2081 (**4a**)[b]	2041 (**4a**)[b]
		1921/2138 (**1b**)[a]	1965/2170 (**1b**)[a]	1882/2126 (**1b**)	1928/2142 (**4b**)[a]	1951/2103 (**4b**)[a]
dsa, Si−H_b	2188 (**1a**)	2190 (**1a**)		2157 (**1a**)[b]	2151 (**4a**)[b]	2134 (**4a**)[b]
		2183/2167 (**1b**)[a]	2183/2165 (**1b**)[a]	2153/2136 (**1b**)	2137/2156(**4b**)[a]	2105/2112 (**4b**)[a]
bdsa, Si−H	1864 (**2a**)	1861 (**2a**)	1926 (**2a**)	1838 (**2a**)	1823 (**6a**)[b]	1851 (**6a**)
			1873/2112 (**2b**)[a]		1817/2083 (**6b**)[a]	
exptl Si−H[c]	1845 (**11c**)	1789 (**11b**)	1793/2012 (**13a**)	1804 (**13b**)		

[a] Left/right value: silyl group close to/far from the metal center. [b] Imaginary frequency of 5i cm^{-1} for **a** → **b** transition. [c] Reference 14.

is found in the C_{2v}-symmetric model complexes **4a**, where the effect amounts to only 0.01 Å. The effect is more pronounced when the smaller alkali metals are relaxed toward one of the Si−H groups to form mono-"agostic" structures **4b**. In this case, the elongation is comparable to that in diagostic **1a**. In the free ligand **5**, the Si−H_a bonds are even shorter than the Si−H_b bonds, thus indicating the apparent influence of the metal. Scheme 2 shows the angle contraction and bond elongation motions.

Compared to the Si−H distances of metal-coordinated silane groups reported in the literature, this elongation of 0.05 Å is rather low. For example, Schubert et al. have used neutron diffraction techniques to characterize some compounds in which R_3Si-H groups seem to be frozen along their path toward oxidative addition to the metal center.[29] They observed elongations up to 0.34 Å. However, in **1** the d^0 configuration of the La^{3+} center precludes metal-to-(Si−H) back-donation, and thus the Si−H_a bond is only slightly weakened.

The N−Si−H_a angle in **1a** is contracted to 101.8°, as compared to the bond angle of the nonagostic N−Si−H_b atom triple of 117.3°. These data express an overall tilt of the SiH_3 group, with the apex of the SiH_3 pyramid pointing not directly to the nitrogen atom to which it is actually bonded, but rather toward the other silyl group. To decide whether the observed angles are due to the influence of an agostic distortion, we compare the data to the structures of model compounds **4** and **5** (Table 1). The nonagostic angle N−Si−H_b is similar in all cases. Hence, the large value of about 117° appears to be typical for the disilylamide fragment and is unaffected by the presence of a metal center. In contrast, the N−Si−H_a angle is gradually contracted when going from the metal-free anion **5** (113.2°) over the sodium (108.0°) and lithium (107.4°) compounds **4a** to the lanthanum complex **1a** (101.8°). Within an ionic model, this can be understood from the increasing Coulomb attraction exerted by the metal due its increasing partial charge. For the bdsa-containing compounds **2** and **3**, similar, yet more pronounced distortions of the local $SiHMe_2$ geometry are observed. Once again, this points to an enhancement of the diagostic interactions due to inclusion of the four methyl groups in the silylamide ligand. The reader is referred to Table 1 for more details.

As already pointed out, the Si−N−Si angle is a sensitive probe of the symmetric La···(Si−H) β-diagostic interaction in **1**. Our calculations on **5** reveal that the free C_{2v}-symmetric disilylamide anion shows an Si−N−Si equilibrium angle of 148.6°. The Si−N−Si angle is *contracted* by 16.5° (13.9°) when the Li^+ (Na^+) ion coordinates symmetrically to free anionic **5**. This can easily be understood from a rehybridization of the bonding orbitals at nitrogen when going from **5** to **4a** according to Bent's rule.[30] In **5**, nitrogen hybridization is between sp^2 and sp, the sp part favoring a linear arrangement. When the alkali cation is coordinated to nitrogen, the p character of the hybrid is increased, or, which is the same in this case, its s character is reduced, allowing for a direct bond to the metal by a hybrid orbital of predominantly sp^2 type. In **1a**, these arguments still hold. However, here the angle does *not* contract as expected from Bent's rule alone, since an additional diagostic interaction forces the Si−N−Si angle to open by 5.9° compared to that in **5**. Thus, assuming the (Si−H)···La interaction as the driving force, this suggests that the agostic interaction is strong enough to distort the Si−N−Si angle of the disilylamide fragment to the extent observed. In the bdsa compounds, the action of the agostic bonds is less obvious, since the Si−N−Si angle of the free anion is almost linear (177.1°). For a simple or even a complex fragment to fit into the tripod bdsa bite, it is necessary to contract the angle due to geometrical requirements.

In summary, we conclude that compounds **1**, **2**, and **3** show conspicuous structural deformations, suggesting the presence of a unique double β(Si−H)···La agostic bond, in good agreement with available experimental data. They are believed to represent excellent models to study the dominant electronic features of the agostic bonding observed in **A**. An excellent structural agreement between theory and experiment is achieved both at the BP86/DZP and BP86/DZP+f levels.

3.2. Vibrational Analysis. Agostic interactions are revealed not only by changes in the local ligand geometries, but also via certain spectroscopic characteristics. They usually lead to a significant weakening of the agostic element hydrogen bonds, which can be seen experimentally from a shift of the E−H stretching vibration to lower frequencies in the vibrational spectrum.[1,10] The calculated harmonic frequencies of the totally symmetric bond stretching vibrations of agostic Si−H_a vs nonagostic Si−H_b groups are collected in Table 2 for complexes of type **1** and **2** with several different central rare earth metals.

From the data in Table 2, it can be seen that the Si−H vibrations for the simple dsa complexes **1** appear at higher frequencies than the experimental bdsa references. Without consideration of any agostic effects, introduction of the four methyl groups into the dsa ligand to yield bdsa leads to a reduction of absolute frequencies, which allows for a direct comparison of the bdsa complexes **2** with experimental data for **A**. While a reasonably good agreement for lanthanum is achieved, the calculated values are somewhat too high for the other central metals.[31] Given the observed dependency of the

(28) (a) Goldfuss, B.; Schleyer, P. v. R.; Handschuh, S.; Hampel, F.; Bauer, W. *Organometallics* **1997**, *16*, 5999−6003. (b) Schleyer, P. v. R.; Clark, T. *J. Chem. Soc., Chem. Commun.* **1986**, 1371−1373. (c) Sekiguchi, A.; Ichinohe, M.; Takahashi, M.; Kabuto, C.; Sakurai, H. *Angew. Chem., Int. Ed. Engl.* **1997**, *36*, 1533−1534.

(29) (a) Schubert, U.; Ackermann, K.; Wörle, B. *J. Am. Chem. Soc.* **1982**, *104*, 7378−7380. (b) Rabaâ, H.; Saillard, J.-Y.; Schubert, U. *J. Organomet. Chem.* **1987**, *330*, 397−413. (c) Schubert, U.; Bahr, K.; Müller, J. *J. Organomet. Chem.* **1987**, *327*, 357−363.

(30) Bent, H. A. *Chem. Rev.* **1961**, *61*, 275−311.

(31) Scaling schemes have been developed to overcome systematic errors in calculated vibrational frequencies. See, for example: Scott, A. P.; Radom, L. *J. Phys. Chem.* **1996**, *100*, 16502−16513. Since we are less interested in absolute values, we did these without scaling, but rather exploited the relative changes in the vibrational frequencies.

Table 3. Natural Atomic Partial Charges (BP86/DZP+f)

atom(s)	**1a** (La)	**1b** (La)[a]	**4a** (Li)	**4b** (Li)[a]	**5**
M	+2.480 (La)	+2.510 (La)	+0.961 (Li)	+0.952 (Li)	
N	−1.859	−1.883	−1.893	−1.868	−1.715
Si	+1.198	+1.158/+1.149	+1.159	+1.162/+1.169	+1.185
H_a	−0.297	−0.276/−0.242	−0.249	−0.304/−0.230	−0.273
H_b	−0.200	−0.194/−0.198	−0.222	−0.217/−0.224	−0.277
SiH_3	+0.501	+0.494/+0.511	+0.466	+0.424/+0.491	+0.358
$N(SiH_3)_2$	−0.857	−0.878	−0.961	−0.952	−1.000

[a] Left/right value: silyl group close to/far from the metal center M.

Si−H vibrational frequencies on the structural details of the complexes,[14] however, the agreement is considered reasonable. The inclusion of rare earth metal f functions in the basis set again only slightly changes the absolute vibrational frequencies to higher values.

More relevant than the absolute numbers is the frequency shift between vibrations of agostic and nonagostic Si−H groups. For the bdsa complexes, such a comparison is possible only for the asymmetric scandium complexes, bearing an agostic and a nonagostic $SiHMe_2$ group in the same complex. Here, the calculated shift of 239 cm^{-1} is in good agreement with the experimental value of 219 cm^{-1}. The simpler dsa complexes **1** allow for the determination of the agostic shift also for the symmetric complexes **1a** by comparison of the Si−H_a and Si−H_b frequencies. Similar shifts between 218 and 251 cm^{-1} are predicted, indicating comparable agostic interactions as in the bdsa complexes.

More information about the agostic interaction itself can be obtained by a comparison of the vibrational data of **1** and **2** with those of the simple models **4a**/**b** and **6a**/**b**. In the C_{2v}-symmetric model compound **4a**, the lithium ion induces a shift of only 70 cm^{-1}, which is significantly smaller than that of the rare earth metals. However, when the lithium ion is allowed to come close to one of the Si−H_a bonds as in C_s-symmetric **4b**, a frequency shift comparable to that in **1a** is observed (209 cm^{-1}). These results suggest that the smaller shift induced by Li^+ in **4a** is due to its smaller size or, more precisely, due to the different electrostatic potential introduced by Li^+. Following the same argument, the sodium ion in **4a** (Na) induces a slightly larger shift of 93 cm^{-1} due to its increased size. In **4b** (Na), however, the reduced ability of the sodium atom to polarize its surroundings results in a smaller frequency shift than in the lithium analogue (154 vs 209 cm^{-1}). Similar arguments hold for the bdsa models **6**. Moreover, in the bdsa complex **2a** (Sc) with the smallest trivalent cation, a Si−H vibrational frequency significantly higher than that for the other rare earth metals is calculated. Again, a larger shift is obtained when the symmetric structure collapses to **2b** (Sc), where the small scandium center is much closer to one of the Si−H groups.

So far, we conclude that the observed frequency shifts induced by the larger and highly charged rare earth metals can be well explained in terms of an electrostatic model.

3.3. Electronic Nature of the *β*-Agostic Ln···(Si−H) Interaction. In this section, we like to shed more light on the origin and electronic nature of the La···(Si−H) *β*-agostic interaction. We will address the question of covalency vs ionicity[15,32] in terms of partial charges and orbital overlap arguments, and we will discuss the contribution of d and f orbitals to the bonding. The structural and spectroscopic data reported so far recommend complexes of type **1** as useful models for studying the electronics of the agostic bonding in **A**. The discussion will take advantage of the fact that, in the dsa complexes **1**, agostic and nonagostic Si−H bonds can be investigated and compared within the same molecular structure. We will then proceed to analyze additional aspects introduced by the more sophisticated bdsa structures **2** and **3**.

Partial Charges. We have performed a natural population analysis (NPA) and natural bond order (NBO) analysis[24] on our prototypical models **1**−**7**. This partitioning scheme has proven to be extremely valuable for the analysis of the electronic structure even of largely ionic compounds, while lacking the major limitations of the traditional Mulliken population analysis. The model cases are compared in terms of partial charges of interacting versus non-interacting hydrogen atoms (H_a vs H_b), silicon and metal atoms, as well as Wiberg bond indexes.[33]

C−H and Si−H agostic bonds may be classified according to their different dipolar structures. In transition metal alkyl complexes, the C−H bond is slightly polarized toward the carbon atom, the hydrogen atom being the more electropositive atom in the ligand fragment.[6] The polarity of the Si−H bond, however, is opposite, the hydrogen atom being the more electronegative partner.[28] Thus, while an electrostatic interaction between the agostic ligand and the metal center in the former type is expected to be due to the carbon−metal attraction, the latter Si−H agostic compounds show a predisposition to interact via the negatively polarized hydrogen atom. Apart from this purely electrostatic model, the accumulation of electron density on the hydrogen atom in Si−H bonds predestines the agostic hydrogen atom to donate into vacant valence orbitals of the electrophilic (Lewis acidic) metal center of the complex. The charge distribution within the three-center Si−H_a···La moiety was studied by inspection of the partial charges calculated for our model systems, which are summarized in Table 3.

The lanthanum atom in **1a** bears a high positive partial charge of +2.48 elementary charges (e), while the nitrogen atom, which is bound directly to the metal center, has a negative charge of −1.86 e. The disilylamido fragment as a whole is charged by −0.86 e, indicating a charge transfer of 0.14 e to the {La(Cp_2-SiH_2)} moiety upon complexation. These results seem to support the common notion that the bonding in rare earth metal complexes is predominantly ionic in character.[15] However, we note here that the transfer of electron density in **1a** is significantly higher than that in the ionic models **4a**.

Clearly, the highly charged lanthanum center is strongly polarizing its surroundings, including the Si−H_a bonds. Thus, the hydrogen atoms H_a which eclipse the lanthanum atom are more negatively charged than their gauche congeners H_b by 0.10 e. On the other hand, this might also suggest that there is no significant transfer of electron density from H_a to the lanthanum center, which would, of course, lead to a more

(32) For studies on LnX_3, see, e.g.: (a) Adamo, C.; Maldivi, P. *Chem. Phys. Lett.* **1997**, *268*, 61−68. (b) Lanza, G.; Fragalà, I. L. *Chem. Phys. Lett.* **1996**, *255*, 341−346. (c) Cundari, T. R.; Sommerer, S. O.; Strohecker, L. A.; Tippett, L. *J. Chem. Phys.* **1995**, *103*, 7058−7063. (d) Di Bella, S.; Lanza, G.; Fragalà, I. L. *Chem. Phys. Lett.* **1993**, *214*, 598−602.

(33) (a) Wiberg, K. B. *Tetrahedron* **1968**, *24*, 1083−1096. (b) Sannigrahi, A. B. *Adv. Quantum Chem.* **1992**, *23*, 301−351.

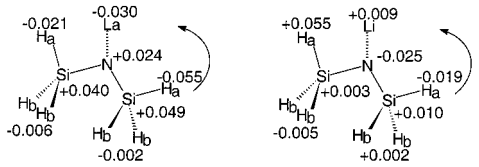

Figure 2. Flow of charge density in **1** (La) and **4** (Li) upon formation of the second agostic bond (negative sign, gain in electron density; positive sign, loss of electron density).

Table 4. Natural Atomic Partial Charges (BP86/DZP+f)

atom(s)	**2a** (La)	**3a** (La)	**6a** (Li)	**6a** (Na)	**7**
M	+2.483	+2.498	+0.921	+0.957	
N	−1.903	−1.905	−1.879	−1.859	−1.797
Si	+1.726	+1.725	+1.713	+1.712	+1.721
H_a	−0.337	−0.332	−0.340	−0.344	−0.299
$SiHMe_2$	+0.533	+0.543	+0.479	+0.451	+0.399
$N(SiHMe_2)_2$	−0.837	−0.818	−0.921	−0.957	−1.000

positive partial charge on H_a compared to that on H_b. However, one has to keep in mind that the charge on the hydrogen atom is, in fact, influenced both by the adjacent silicon atom to which it is bound covalently and by the proximity of the metal center due to the agostic interaction. Hence, the negative partial charge on H_a, as compared to that on H_b, does not necessarily rule out the possibility of charge transfer to the lanthanum atom, although the ionic contribution seems to predominate. A similar polarization of the Si−H_a electron density by the metal is observed in the ionic models **4a** and **4b**.

The *asymmetric* structure **1b** allows for a comparison of a nonagostic (far from the metal) and an agostic (close to the metal) silyl group (Table 3) and the change in partial charges upon formation of the second agostic bond (Figure 2). The results are in line with the interpretation given above, the agostic SiH_3 group showing a stronger negative polarization toward the lanthanum center than the nonagostic one. As indicated before, the electrostatic polarization of the disilylamide fragment obscures any charge-transfer effects from the Si−H_a bonds to the La center. Still, as can be derived from the data in Table 3, electron density of 0.02 e is transferred from the $\{N(SiH_3)_2\}$ ligand to the $\{La(Cp_2SiH_2)\}$ moiety upon formation of the second agostic bond (**1b** → **1a**). This is in contrast to the changes observed on going from **4b** (Li) to **4a** (Li), where the lithium atom instead *loses* part of its residual electron density. The charge rearrangement within the disilylamide fragment is clearly dominated by electrostatic factors in this case. We restrict ourselves here to stress that the flow of charge density during the transformation **1b** → **1a** is qualitatively distinct from that in the **4b** → **4a** case (Figure 2).

The charge distribution in the bdsa complexes **2a** and **3a** is similar to that in the simpler model **1a** (Table 4). The overall transfer of electron density from the bdsa ligand to the metal-containing complex fragment is slightly higher in **2a** and **3a** than that in **1a**, and significantly higher than that in the purely ionic models **6a** (Li, Na). Still, the agostic hydrogen atoms are more negatively charged than those in **1a**, but less negative than those in **6a** (Li, Na). The partial charge of the central rare earth metal is similar in the three complexes **1a**, **2a**, and **3a**. These data, in summary, point to a more pronounced agostic bonding in the bdsa complexes compared to the simpler dsa complexes. On the basis of the charge distribution, nonelectrostatic contributions to the agostic bonding cannot entirely be ruled out.

Covalent Bond Orders. Another hint to answering the question of ionicity vs covalency can be obtained by inspection of the Wiberg covalent bond order matrixes calculated in the natural atomic orbital (NAO) basis for our model structures, which are partially recorded in Table 5.

Table 5. Wiberg Bond Orders in the NAO Basis (BP86/DZP+f)

atom pair	bond order **1a**	**2a**	**3a**	atom pair	bond order **1b**[a,c]
La, H_a	0.040	0.052	0.045	La, H_a	0.030/0.016
La, H_b	0.006			La, H_b	0.006/0.005
Si, H_a	0.820	0.764	0.774	Si, H_a	0.846/0.883
Si, H_b	0.897			Si, H_b	0.901/0.905
La, Si	0.031	0.034	0.032	La, Si	0.030/0.022
La, N	0.143	0.151	0.133	La, N	0.154
La, C[b]	0.065	0.069	0.065	La, C[b]	0.071

atom pair	bond order **4a** (Li)	**6a** (Li)	**6a** (Na)	atom pair	bond order **4b** (Li)[a]	**6b** (Li)[a]
M, H_a	0.002	0.033	0.013	M, H_a	0.015/0.007	0.022/0.001
M, H_b	0.002			M, H_b	0.002/0.002	
Si, H_a	0.893	0.777	0.791	Si, H_a	0.843/0.905	0.782/0.862
Si, H_b	0.893			Si, H_b	0.885/0.898	
M, Si	0.005	0.018	0.009	M, Si	0.013/0.004	0.016/0.005
M, N	0.062	0.048	0.030	M, N	0.062	0.057

[a] Left/right value: silyl group close to/far from the metal center. [b] Carbon atom in the cyclopentadienyl rings; mean value. [c] Geometry optimized at BP86/LanL2DZ.

In general, the Si−H bonds are characterized by covalent bond orders (b.o.) close to 1 (SiH_3 b.o. ≈ 0.9; $SiHMe_2$ b.o. ≈ 0.8), while ionic dominance is attributed to the La−N bond (b.o. ≤ 0.154). The covalent bond indexes for La···H and La···Si are close to 0 (b.o. ≤ 0.052). Still, in **1a**, the agostic hydrogen atoms H_a show a noticeably higher bond order with the lanthanum center as compared to the nonbonding gauche H_b···La values, the absolute magnitude of the former being comparable to that of the Cp ring carbon atoms bonding to the lanthanum center. The difference in La···H_a bond orders between the agostic and nonagostic Si−H groups in **1a** and **1b** is small, but still distinguishable. The corresponding Si−H_a bonds are slightly weakened compared to the Si−H_b bonds, which might be rationalized by a charge transfer of Si−H_a bonding density to the electronically unsaturated metal center. A similar change in Si−H_a bond orders is also induced by the Li^+ ion when it is allowed to come close to one of the SiH_3 groups, like in **4b** (Li). However, in contrast to the larger La^{3+} center, the Li^+ ion is too small to significantly reduce the Si−H_a bond orders when it is forced to take a central position, as in **4a** (Li). While a negative polarization of H_a just as in the lanthanum complex is still observed, a concomitant increase in covalent bond order for the interaction between Li and H_a over H_b cannot be distinguished in **4a**, contrasting the La···$H_{a/b}$ interactions in the lanthanum complex **1a**. In summary, however, these data attribute only a very small covalent contribution to the agostic La···H_a interaction in **1**.

The situation is not very much different for the more realistic bdsa complexes **2a** and **3a**. La···H bond orders are only very slightly increased in these structures, while the La···Si values remain virtually unchanged with respect to **1a**. Overall, in agreement with other criteria reported so far, the agostic bonds appear to be somewhat stronger in **2a** than those in **1a** and **3a** and considerably stronger than those in the ionic models **6a** (Li, Na).

Natural Bond Orbital Interaction. An analysis of the interaction between the natural bond orbitals by second-order perturbation theory shows a stabilizing donor−acceptor interaction via the occupied, localized Si−H_a bond orbital to a vacant lanthanum-centered sd^2 hybrid orbital (Table 6). This leads to a stabilization of approximately 3.2 kcal/mol due to each of

Table 6. Dominant Agostic Bonding Contributions According to Perturbation Theory (PT2) in the NBO Basis

interaction	**1a** (La): σ(Si−H) → La	**4b** (Li): σ(Si−H) → Li
PT2-energy[a] (kcal/mol)	3.2	3.0
donor hybrids	34.7%: Si s (20.5%), p (78.4%), d (1.1%) 65.3%: H s (99.9%), p (0.1%)	34.7%: Si s (20.1%), p (78.8%), d(1.1%) 65.3%: H s (99.9%), p (0.1%)
acceptor hybrids	La s (31.1%), p (0.4%), d (67.7%), f (0.8%)	Li s (86.6%), p (11.4%), d (2.0%)
interaction	**2a** (La): σ(Si−H) → La	**6b** (Li): σ(Si−H) → Li
PT2-energy[a] (kcal/mol)	5.4[b]	5.1
donor hybrids	32.1%: Si s (18.4%), p (80.4%), d (1.3%) 67.9%: H s (99.9%), p (0.1%)	32.0%: Si s (18.1%), p (80.5%), d (1.4%) 68.0%: H s (99.9%), p (0.1%)
acceptor hybrids	La s (46.6%), p (0.3%), d (52.5%), f (0.7%) La s (0.7%), p (1.1%), d (97.7%), f (0.6%)	Li s (86.9%), p (11.4%), d (1.8%)

[a] Interaction energy per agostic bond. [b] **3a** (La): 8.0 kcal/mol.

Table 7. Selection of High-Energy Occupied Kohn−Sham MO's Involved in Agostic Bonding of **1a**

number	symmetry	orbital energy[a]	bonding character[b]	principal components
52	b_2	−0.21219	ab: La−N/ab: La···H_a	La(p_y, d_{-1})/N(p_y)
50	a_1	−0.22143	b: La···H_a/ab: La−N	La(p_z, d_{+2})/N(p_z)/H_a(s)
48	a_1	−0.25099	b: La···H_a/b: La−N	La(d_0)/N(p_z)/H_a(s)
43	b_2	−0.32190	nb: La···H_a/nb: La−N	La(p_y, d_{-1})/N(p_y)/H_a(s)/Si(p_y, p_z)
39	a_1	−0.34212	nb: La···H_a/ab: La−N	La(p_z, d_{+2})/N(p_z)/H_a(s)/Si(p_z)
32	a_1	−0.36058	ab: La···H_a/ab: La−N	La(s)/N(p_z)/H_a(s)/Si(p_z)

[a] Hartrees. [b] Abbreviations: b = bonding; nb = nonbonding; ab = antibonding.

the agostic bonds in **1a**. There is no significant participation of f orbitals. A similar interaction of 3.0 kcal/mol stabilizes **4b** (Li; 1.6 kcal/mol for Na). Here, the lithium-centered acceptor NBO has predominantly s character, while the Si−H donor NBO is essentially the same as that in **1a** (La). This interaction essentially vanishes (i.e., <0.1 kcal/mol) in **4a** (Li), obviously since the small Li^+ ion is not capable of simultaneously forming two agostic bonds. For the somewhat larger sodium cation, the interaction is as weak as 0.25 kcal/mol.

As expected, somewhat stronger agostic bonds are attributed to the bdsa complexes, while the nature of the interaction is virtually identical to the one reported for **1a** (Table 5). In **2a**, interactions of two acceptor orbitals of pure d and sd type with a Si−H bonding orbital sum up to 5.4 kcal/mol on average per agostic bond. In **3a**, the situation is comparable but more complicated, since at least five acceptor orbitals contribute to the bonding.[34] Interestingly, the relevant orbital interactions in **3a** result in an interaction energy of 8.0 kcal/mol on average per agostic bond. This may seem somewhat surprising, given the results reported previously in this paper, where the agostic bonding in **3a** appeared weaker than that in **2a**. We therefore recommend a careful interpretation of the absolute interaction energies reported here, but rather stress that agostic bonding in the bdsa complexes is stronger than that in the dsa compounds.

The ionic models **6a** (C_{2v}-symmetry) lead to lower interaction energies (2.3 kcal/mol for Li, 1.9 kcal/mol for Na). Only in the C_s-symmetric case **6b** (Li), where a close interaction of the alkali metal with the Si−H moiety is possible, is a comparable stabilization of 5.1 kcal/mol for the single agostic bond gained.

No significant stabilizing back-donation of metal electrons to the disilylamide moiety is predicted, as expected for a d^0 transition metal ion.[35] According to the analysis in the picture of localized orbitals, the agostic interactions in complex **1a** can be described as a double three-center, two-electron bond, paralleling the description of Brookhart and Green for agostic compounds of the C−H type.[1]

Table 8. Coefficients of Basis Functions Composing Molecular Orbitals 43, 48, 50, and 52

molecular orbital	atom-centered basis function coefficients		
	La	H_a	N
43	p_y 0.11, 0.01 d_{-1} −0.09, −0.04	s 0.21, 0.26	p_y 0.22, 0.05
48	d_0 −0.27, −0.07 f_0 −0.02	s 0.09, 0.16	p_z 0.46, 0.25
50	p_z 0.24, −0.06 d_0 0.03, 0.07 d_{+2} −0.13, −0.08 f_0 −0.02	s 0.05, 0.09	s −0.02, −0.09 p_z 0.30, 0.20
52	p_y 0.18, 0.10 d_{-1} 0.20, 0.06 f_{-3} 0.02	s 0.01, 0.01	p_y 0.02, 0.00

Analysis of the Canonical Kohn−Sham Molecular Orbitals. Inspection of the canonical Kohn−Sham molecular orbitals (MOs) of complex **1a**[36] reveals the presence of several doubly occupied MOs which lead to a buildup of electron density between the metal center and the hydrogen atoms (Table 7). The a_1-symmetric agostic molecular orbital number 48, occurring at −0.25099 hartrees, is mainly composed of a lanthanum-centered d_0 (i.e., $l = 2$, $m_l = 0$) orbital, with a small admixture of f_0, which overlaps with a nitrogen p_z orbital and s orbitals centered at the agostic hydrogen atoms (Figure 3b). Within this MO, the lanthanum d coefficients and the hydrogen s coefficients both are comparably high, indicating some degree of polar covalent bonding (Table 8). A similar conclusion can be drawn from molecular orbital number 50 (a_1, −0.22143 hartree), which documents a constructive overlap of a lanthanum p−d hybrid with hydrogen s orbitals (Figure 3c). It is antibonding between the lanthanum and nitrogen atoms. A somewhat more ionic contribution to the bonding is suggested by molecular orbital number 43, which transforms as the b_2 irreducible representation of the point group, due to the rather high

(34) We note that two of the five agostic acceptor orbitals in **3a** (La) contain an f participation of 3%, while contributions of <1% were found in any other relevant orbital. The energetic contributions of the corresponding donor−acceptor interactions are as low as 0.5 kcal/mol, however.

(35) In fact, weak back-bonding interactions from the metal to the antibonding Si−H orbital are found in **3a** (La) and **6a** (Li), with a stabilizing energetic contribution of 0.18 and 0.23 kcal/mol per agostic bond, respectively.

(36) The MO's discussed in section 3.3 were obtained from a separate calculation using the DZP+f basis set on structure **1a** with exact C_{2v} symmetry (BP86/DZP+f). The shapes of the molecular orbitals for **2a** and **3a** do not reveal any additional information and are thus not discussed.

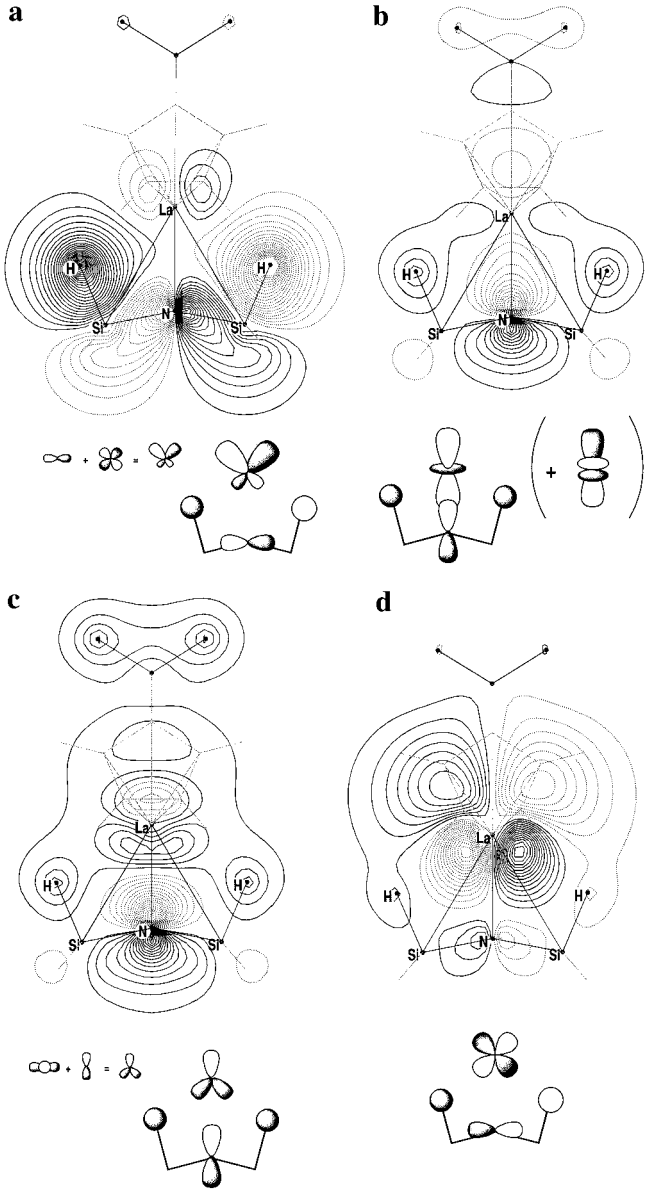

Figure 3. Selection of high-energy occupied Kohn−Sham MO's involved in agostic bonding of **1a**; schematic representation of principal components. (a) Orbital number 43; $\epsilon_{43} = -0.32190$ hartree; b_2. (b) Orbital number 48; $\epsilon_{48} = -0.25099$ hartree; a_1. (c) Orbital number 50; $\epsilon_{50} = -0.22143$ hartree; a_1. (d) Orbital number 52; $\epsilon_{52} = -0.21219$ hartree; b_2.

coefficients of the hydrogen s functions compared to lanthanum p,d orbital coefficients (Figure 3a).

However, there are also several occupied antiagostic molecular orbitals present in **1a**, i.e., which are interfering destructively between lanthanum and agostic hydrogen atoms. One of them is shown in Figure 3d (number 52, b_2), which represents an antibonding La−N interaction as well as an antibonding La···H interaction. The balance of bonding vs antibonding MOs can be viewed as one factor that energetically prevents the system from intensifying one of the agostic bonds while breaking the other one in favor of an asymmetric structure **1b**.

The coefficients of the f basis functions range between 0.025 and 0.01 in orbitals 43, 48, 50, and 52, while being invariantly lower in all the other occupied MOs.[37] The unoccupied MOs

(37) A maximum f coefficient of 0.035 is obtained in the HOMO of **3a** (La).

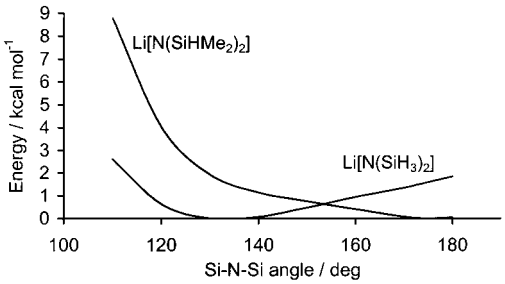

Figure 4. C_{2v} symmetric Si−N−Si angle bending potential for **4a** (Li) and **6a** (Li).

of predominantly f character at lanthanum occur at very high energy and do not contribute to the bonding. We therefore attribute the role of f functions as polarization functions, which only slightly adjust the shape of occupied orbitals and electron density without changing their character significantly. This is in accord with the results reported in previous sections. The situation may be different for other lanthanide central metals with nonzero f orbital population, however.

3.4. Energetics of Agostic Bonding. We now deal with the question of how strong the agostic interaction with the lanthanum and other lanthanide metal centers in **A** and the models **1** (La) and **2** (La) actually is. The answer to this provides an approximate energetic measure of how strongly a coordination site at the metal center is blocked by the agostic interaction in these complexes, which is of significance for their reactivity.

A clue to this question has already been given in the last section within the NBO picture (Table 6). While the dominant orbital interaction energy in **1a** (La) is as low as 3.2 kcal/mol per agostic bond, the binding in the more realistic models **2a** (La) and **3a** (La) amounts to 5.4 and 8.0 kcal/mol, respectively. These numbers, however, do not necessarily reflect the true dissociation energies per agostic bond, which is a superposition of roughly two effects, namely the bending potential of the Si−N−Si angle and the agostic bond itself.

A decomposition of these effects can be achieved via calculation of the Si−N−Si angle bending potential in a disilylamide complex where the overall electronic situation is similar to that in **1** or **2**, but where no dominant agostic bonding is present. Model compounds **4a** (Li) and **6a** (Li) are expected to meet these requirements to a sufficient level of approximation. Figure 4 shows the relaxed Si−N−Si angle bending potential (calculated in C_{2v} symmetry) for the model compounds **4a** (Li) and **6a** (Li).

The Si−N−Si bending potential of lithium disilylamide **4a** (Li) shows a minimum at 132°. The calculation reveals that the potential curve is rather flat, with an energy difference of only 0.7 kcal/mol for angles of 130° and 155°, suggesting an extraordinarily flexible Si−N−Si angle in nonagostic disilylamide complexes.[38] Clearly, this allows for the large angle distortions observed experimentally and in the calculations, with rather weak interactions sufficing as the driving forces. The Si−N−Si bending potential for lithium bis(dimethylsilyl)amide **6a** (Li), however, is qualitatively distinct from that of **4a**. Its minimum is located at 176°, and the force constant is even lower than that in **4a**. In the range from 180° to 125°, the potential is also very flat, indicating very low repulsive forces against angle

(38) A sufficient flexibility of the silicon basis set is essential for a correct description of the potential. For instance, omission of the d polarization functions on silicon stiffens the potential at high Si−N−Si angles. Hence, it is clear why a monoagostic structure **1b** (La) as reported in section 3.1. is only artificially stable in calculations with the limited LanL2DZ basis set.

Table 9. Selected Structural Parameters for Model Complexes **1**, **2**, and $[CpScN(SiH_3)_2]^+$ in Angstroms and Degrees (BP86/DZP+f)

complex	∠Si−N−Si	Si−H_a	Si−H_b	∠H_a−Si−N	∠H_b−Si−N	M···H_a	M···Si_{bridge}
1b (Sc)	134.3	1.534/1.492	1.489/1.492	99.7/108.8	118.0/113.2	2.27/3.51	3.324
1a (Y)	160.4	1.539	1.488	101.1	117.4	2.47	3.435
1b (Y)	136.5	1.534/1.497	1.489/1.492	100.4/107.6	118.2/114.0	2.42/3.46	3.437
1a (La)	154.5	1.536	1.488	101.8	117.3	2.68	3.604
1a (Lu)	158.1	1.548	1.498	100.4	117.5	2.49	3.417
$[CpSc(N(SiH_3)_2)]^+$	159.9	1.546	1.463	94.2	116.7	2.20	
2a (Sc)	161.5	1.542		98.5		2.32	3.357
2b (Sc)	141.4	1.554/1.502		96.9/105.7		2.18/3.25	3.341
2a (Y)	163.4	1.555		99.2		2.38	3.447
2a (La)	158.2	1.553		100.0		2.58	3.599

contraction and high flexibility of the ligand. Below 125°, the potential shows a steeper slope, possibly due to steric (closed-shell) repulsion of the methyl groups. Compared to **4a**, this repulsive flank appears already at higher Si−N−Si angles due to the increased bulkiness of the methyl groups. Thus, in contrast to the simple dsa ligand, the bdsa ligand by itself prefers high Si−N−Si angles and thus favors the formation of diagostic bonds as observed in **2**, **3**, and **A**. In the model complexes **1**, however, the Si−N−Si bending potential impedes to some extent the formation of the diagostic bond since its minimum is located at lower angles. Thus, summing up the contributions from the Si−N−Si angle deformation (ca. 0.7 kcal/mol) and the agostic interaction energy derived by the NBO analysis (3.2 kcal/mol), an agostic dissociation energy of 2.5 kcal/mol results for the simple model **1a** (La).

The same number can be obtained in a more direct fashion by calculating the energy difference of the symmetric diagostic interaction (**1a**, C_{2v}) and the situation in which one agostic bond is broken (**1b**, C_s). At the BP86/DZP+f level, the energy difference between **1a** and **1b** (optimized at BP86/LanL2DZ) amounts to 2.6 kcal/mol, which is close to the above estimate. For the more realistic models **2a** and **3a**, the NBO perturbation theory values of 5.4 and 8.0 kcal/mol, respectively, may provide useful estimations for the agostic bond dissociation energies due to the different shape of the bdsa potential. The variance in the values for **2a** and **3a**, however, remains unexplained at this time, and for this reason we must handle the absolute values with some care. Moreover, the dissociation energies are expected to be sensitive to the nature of the Cp ring substituents, mainly due to steric constraints.

Agostic dissociation processes such as the one analyzed above may have important consequences for the chemical behavior and reactivity of the complexes **A**. One of the major advantages of the "extended silylamide route" using bdsa ligands is the enhanced yield of THF-adduct-free complexes.[14] This is easily rationalized if one considers that the dissociation of THF from the complex is facilitated by competitive formation of an agostic bond of comparable binding strength.[39] Moreover, even smaller energy differences such as that calculated for **1a** (La)/**1b** (La) readily explain why no experimental evidence for monoagostic species with the larger metals could be found in solution at ambient temperature so far.

3.5. The Effect of Metal Size. We have seen that a symmetric diagostic interaction is favorable for a central metal ion as large as lanthanum. However, a similar coordination mode has not been observed for all rare earth complexes of type **A**.[14] We have therefore studied the occurrence of symmetric Ln···(Si−H) β-diagostic bonding in complexes of type **1** and **2** in the series La−Y−Sc−Lu. The most important parameter at change is the ionic radius of the rare earth metal in the complex and, in the case of La, the presence of low-lying vacant f orbitals. The results of our calculations are summarized in Table 9 and visualized in Figure 5. Vibrational frequencies are given in Table 2.

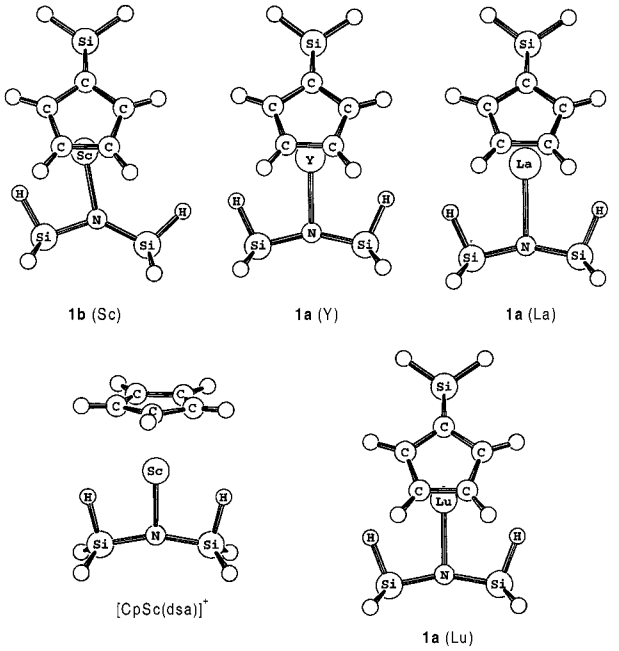

Figure 5. Optimized geometries of **1b** (Sc), **1a** (Y), **1a** (La), **1a** (Lu), and $[CpSc(N(SiH_3)_2)]^+$.

Similar to the case for the lanthanum complex, we find the symmetric diagostic interaction to be a stable coordination mode in the case of the simplest yttrium complex **1a** (Y). Additionally, an asymmetric structure **1b** (Y) was found to be a stable minimum, which is only 0.58 kcal/mol higher in energy than **1a** (Y). For scandium, however, only an asymmetric monoagostic coordination mode **1b** (Sc) could be located. For the lutetium complex, only **1b** (Lu) is calculated to be a true minimum, while the symmetric structure **1a** (Lu) turns out to be a first-order saddle point, with a very low imaginary frequency of only 5i cm^{-1} for the conversion **1a** (Lu) → **1b** (Lu). As for **1** (Y), the energetic difference between both coordination modes is very low (0.56 kcal/mol). In summary, for the simple model **1**, both mono- and diagostic structures have been observed for Y and Lu, while La and Sc exhibit only the symmetric diagostic or the asymmetric monoagostic mode, respectively. The apparent similarity of the Y and Lu complexes parallels that of their ionic radii (0.900 Å for Y^{3+}, 0.861 Å for Lu^{3+}; coordination number 6).[40]

(39) THF dissociation energies have been reported to be around 10 kcal/mol, cf.: Nolan, S. P.; Stern, D.; Marks, T. J. *J. Am. Chem. Soc.* **1989**, *111*, 7844−7853.

(40) Shannon, R. D. *Acta Crystallogr. A* **1976**, *32*, 751−767.

The details of these mono-/diagostic equilibria are expected to be sensitive to changes in electronics and steric congestion in the compounds. Although a full study of these aspects is out of the scope of this report, it is worthwhile to note that methyl substitution on the dsa ligand to yield the bdsa complexes changes the situation qualitatively. Thus, the symmetric diagostic coordination mode now is the only stable geometry that could be located in the yttrium complex **2** (Y), in contrast to the situation for **1** (Y). For the scandium complex, *both* mono- and diagostic equilibrium geometries **2a** (Sc) and **2b** (Sc) were found, while only a monoagostic mode **1b** (Sc) was detected. These findings again document the greater tendency to form the double agostic bond in the bdsa complexes **2** as compared to **1**, which may be explained by stronger agostic bonds and steric Me−Me repulsion within the bdsa ligand. The increased strength of agostic bonding in the bdsa complexes **2** can also be anticipated from the structural deformations (Table 9), as was corroborated for the lanthanum case. The occurrence of mono- or diagostic species and the strength of agostic bonding is also expected to be dependent on the steric bulk of substituents on the cyclopentadienyl rings of **A**, which may interact in a repulsive manner with the methyl groups of the bdsa ligand, thus disfavoring the formation of agostic interactions. We will not study this important aspect in any detail here, but at this stage rather we will discuss the influence of the central metal itself.

Metal size can have several effects on the tendency to form a symmetric diagostic interaction. In general, a reduction of ionic radius reduces the surface area around the metal ion, thus limiting the available space for ligand coordination. A diagostic coordination of the disilylamide (dsa, bdsa) moiety formally uses three coordination sites and is therefore less probable for small cations. Moreover, the geometric ligand distortions, including the Si−N−Si angle deformation, are expected to be more pronounced in order to facilitate two agostic bonds around a small central metal. This can be seen from a comparison of the calculated structures of the lanthanum and the yttrium complexes (Table 9). The Si−N−Si angles are opened even more for the yttrium complexes than for the lanthanum case. Also, the Si−H_a bond stretching and N−Si−H_a angle contraction are more pronounced for the smaller cation. This is, of course, favored by the larger electrostatic potential of the yttrium ion due to its increased charge/radius ratio, but it might also be a necessary *geometrical* condition to accommodate to the small metal size.

The effect of increased steric strain[41] in the ligand sphere due to the reduced metal size can be seen from Figure 5. With decreasing size, the metal intrudes deeper into the *ansa*-Cp_2-SiH_2 moiety. Numerically, this is reflected by the decreasing distance between the central metal and the *ansa*-bridging Si atom in the sequence La ≫ Y > Lu ≫ Sc (Table 9). As a consequence, the repulsive forces between the Cp rings and the silyl groups of the dsa/bdsa ligand increase from the lanthanum complex to the scandium complex. This may be the reason for the lower tendency of the scandium complex to form a diagostic bond or, viz., to stay in a monoagostic mode. To rule out prohibition by bare metal size as mentioned above, we optimized another model complex (constrained to C_{2v} symmetry), cationic cyclopentadienyl scandium disilylamide, in which steric ligand repulsions should be a minimum. As can be seen from Figure 5 and Table 9, the symmetric diagostic coordination mode like in **1** (La, Y) or **2** (La, Y, Sc) is, in fact, also possible for the simple disilylamide ligand in combination with a small cation such as scandium. As expected, the Si−N−Si angle (159.9°) is predicted to be wider than that in **1b** (Sc) and even that in **1a** (La), and the deformations of the agostic SiH_3 groups are very pronounced. However, due to the overall positive charge of the model complex, the attractive *electrostatic* force exerted on the Si−H_a bonding electrons is much higher than that in the reference complexes under discussion.

The importance of metal size and/or steric congestion can more indirectly be deduced from experimental data. For instance, the steric interaction of the silylamide ligand and the benzo-substituted cyclopentadienyl rings in the isolated lutetium complex *rac*-**15e** leads to a crystallographically disordered $SiHMe_2$ moiety.[14]

The observation that, in general, the lighter rare earth cations are also able to form similar β(Si−H) diagostic interactions as lanthanum, depending on steric interligand repulsion, confirms our conclusion that f orbitals play only a minor role in the bond formation in the cases considered here. In summary, we conclude that the size and accessibility of the coordination area around the central metal play a decisive role in determining the dominance of either species in the equilibrium **1/2a** (Ln) ⇌ **1/2b** (Ln).

4. Conclusion

Structural peculiarities predicted with the aid of current density functional theory (DFT) methods provide evidence for an unprecedented symmetric Ln···(Si−H) β-diagostic interaction between the rare earth metal center and the disilylamide moiety in the model complexes *ansa*-[$(C_5H_4)_2SiH_2LnN(SiHR_2)_2$] (Ln = La, Sc, Y, Lu; R = H, Me). The optimized geometries are in excellent agreement with available experimental data. Similarly, the frequency shift of the isolated Si−H stretching vibration of the silylamide ligand, which is normally observed for agostic groups, is well reproduced by theory. The characteristic weakening of the agostic Si−H bonds is paralleled by a decrease in the covalent bond order, while the lanthanum hydrogen bond order is only slightly increased to a value comparable to that of the La···Cp interaction in metallocenes. The electrons in the Si−H bond are polarized toward the H atom due to the influence of the positively charged lanthanum center, resulting in a more negative partial charge of the agostic hydrogen atoms. This points to a significant electrostatic contribution to the bonding. Molecular and electronic structure data suggest a stronger bond in the $N(SiHMe_2)_2$ (bdsa) than in the $N(SiH_3)_2$ (dsa) complexes.

Analysis of NBO orbitals describes the agostic interaction as a donation of electron density from the Si−H bond to an empty d orbital centered at lanthanum. No significant participation of f orbitals can be devised. The interaction yields a binding energy of about 3.2 kcal/mol per agostic interaction for the dsa complex, which is considerably increased to approximately 5 kcal/mol for the bdsa complexes. The formation of a diagostic bonding mode is supported by a rather flat Si−N−Si angle bending potential, allowing for the unusually wide angles observed in the complexes.

An analysis of the occupied canonical Kohn−Sham molecular orbitals suggests a small covalent contribution to the agostic bonding, which is probably induced by a polarization of the Si−H bonding electron density due to the electrostatic potential of the rare earth metal ion. f orbitals do not seem to play a dominant role in the agostic bonding for the complex type studied here, which is underlined by the occurrence of a similar diagostic interaction in model complexes of the lighter rare earth

(41) (a) Cooper, A. C.; Clot, E.; Huffman, J. C.; Streib, W. E.; Maseras; F.; Eisenstein, O.; Caulton, K. G. *J. Am. Chem. Soc.* **1999**, *121*, 97−106. (b) Ujaque, G.; Cooper, A. C.; Maseras, F.; Eisenstein, O.; Caulton, K. G. *J. Am. Chem. Soc.* **1998**, *120*, 361−365.

metals scandium and yttrium. The details of the mono-/diagostic equilibrium sharply depend on metal size and agostic binding strength. A diagostic mode is less favorable for the smaller rare earth cations. The formation of a diagostic interaction thus seems to be markedly affected by ancillary ligand constraints or metal size effects, emphasizing the principle of steric saturation/unsaturation in organo-f-element chemistry.

Acknowledgment. This work was supported by the Bayerische Forschungsstiftung (Bayerischer Forschungsverbund Katalyse, FORKAT) and the Deutsche Forschungsgemeinschaft. We are grateful for computer time granted by the Leibniz-Rechenzentrum of the Bavarian Academy of Sciences in München.

Supporting Information Available: Optimized structures in Cartesian coordinates and associated total energies; further information on the performance of basis sets and density functionals (PDF). This material is available free of charge via the Internet at http://pubs.acs.org.

JA993421T